RESEARCH ARTICLE
doi: 10.2306/scienceasia1513-1874.2016.42.397

ScienceAsia 42 (2016): **397–406**

Charge-transfer interactions between nitrogen moieties as a basis for different drugs with a picric acid acceptor

Moamen S. Refat[a,b,*], Hosam A. Saad[a,c], Hala Eldaroti[d], Abdel Majid Adam[a], Mohamed A. Al-Omar[e], Ahmed M. Naglah[e,f]

[a] Department of Chemistry, Faculty of Science, Taif University, Al-Haweiah, P.O. Box 888, Zip Code 21974, Taif, Saudi Arabia
[b] Department of Chemistry, Faculty of Science, Port Said University, Port Said, Egypt
[c] Department of Chemistry, Faculty of Science, Zagazig University, Zagazig, Egypt
[d] Department of Chemistry, Faculty of Education, Alzaeim Alazhari University, Khartoum, Sudan
[e] Department of Pharmaceutical Chemistry, Drug Exploration & Development Chair, College of Pharmacy, King Saud University, Riyadh 11451, Saudi Arabia
[f] Peptide Chemistry Department, Chemical Industries Research Division, National Research Centre, 12622-Dokki, Cairo, Egypt

*Corresponding author, e-mail: msrefat@yahoo.com

Received 27 Feb 2016
Accepted 30 Dec 2016

ABSTRACT: The present study investigated and compared the complexation properties of different nitrogen moieties as donors with picric acid as the acceptor. The moieties were triethylamine (TEA), hydrazine (Hyd), thiosemicarbazide (TSC), phenylhydrazine (Phy), and pyridine (Pyr). The composition and stoichiometry of the synthesized complexes were verified by spectrophotometric titration and elemental analysis. The formed complexes were characterized using IR, Raman, ^{1}H NMR, and UV-Vis spectroscopy, and CHN elemental analysis. Thermogravimetric experiments were carried out to investigate the thermal properties of the complexes. The microstructure properties of these complexes were investigated using optical light microscope (OLM). The donation from the nitrogen moieties to the picric acid acceptor in decreasing order was found to be Hyd > TEA > TSC > Phy > Phr. Interestingly, the thermal degradation of the TSC complex led to sulphur atoms remaining as a final residual. The OLM micrograph patterns indicate the formation of high quality coloured crystals.

KEYWORDS: nitrogen moiety, CT complexation, spectroscopy

INTRODUCTION

During the last two decades, numerous studies have been reported on charge-transfer (CT) or proton-transfer interactions. This is owing to their significant chemical and physical properties. CT interaction was first introduced by Mulliken[1] and has been widely discussed by Foster[2]. Mulliken[3] demonstrated that the CT interactions within a molecular complex that consists of an electron acceptor, A, and an electron donor, D, involve a resonance with a transfer of charge from D to A. The CT complexation is of great importance in chemical reactions, including condensation, substitution, and addition[4], drug-receptor binding mechanisms, biological systems[5], bioelectrochemical and biochemical energy-transfer processes[6]. The CT complexation of drugs is an important technique that is simpler, cheaper, and more efficient than many methods of drug determination described in the literature. Furthermore, the study of this complexation may be useful in understanding the mechanism of drug action and the drug-receptor interactions[7–10]. CT complexation is also of great importance in many applications and fields, such as surface chemistry, electrically conductive materials, organic semiconductors, second-order nonlinear optical activity, and in nonlinear optical material[11–14]. As part of our continuing interest in investigating CT interactions, synthesis, characterization, and applications[15–18], we focused this current study on the following objectives: (1) synthesize the CT complexes of picric acid (PA) acceptor with different nitrogen moieties (TEA, Hyd, TSC, Phy, and Pyr); (2) obtain the complexation stoichiometry using spectrophotometric titration and CHN elemental analysis; (3) calculate the spectroscopic data using the 1:1 and 1:2 Benesi-Hildebrand equations; (4) characterize the synthesized complexes

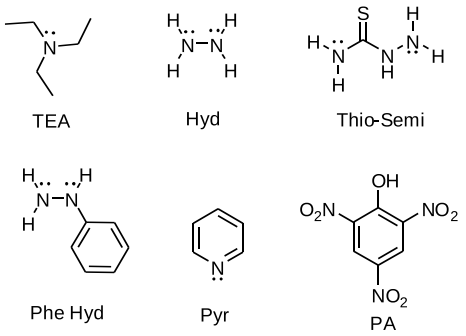

Fig. 1 Chemical structure of nitrogen moieties and the PA acceptor.

structurally via IR, Raman, ^{1}H NMR, and UV-Vis spectroscopy; (5) study the thermal decomposition behaviour of the reported complexes using thermogravimetric analysis; (6) determine the kinetic-thermodynamic parameters (E^*, A, ΔS^*, ΔH^*, and ΔG^*) using Coats-Redfern and Horowitz-Metzger equations; and (7) observe the microstructure characteristics of the reported complexes using OLM technique.

MATERIALS AND METHODS

Reagents

All the reagents used were of high analytical grade chemicals and were used as purchased. Triethylamine (TEA; $C_6H_{15}N$; 101.19), hydrazine (Hyd; N_2H_4; 32.05), thiosemicarbazide (TSC; CH_5N_3S; 91.14), phenylhydrazine (Phy; $C_6H_8N_2$; 108.14), pyridine (Pyr; C_5H_5N; 79.1), and picric acid (PA; $C_6H_3N_3O_7$; 229.1) (Fig. 1) were supplied by Sigma-Aldrich Chemical Company (USA). Methanol of HPLC grade was from E. Merck (Darmstadt, Germany).

Solutions

Standard stock solutions of the PA acceptor and each donor (5.0×10^{-3} M) were prepared by dissolving precisely weighed quantities in a 100 ml volumetric flask using methanol as a solvent. The solutions were protected from light. Solutions for the spectroscopic measurements were made by mixing appropriate volumes of stock solutions with the solvent.

Synthesis

The synthesis procedure is summarized as follows. Two mmol of each donor (20 ml) was added to 20 ml of methanolic solutions containing PA (2 mmol) and stirred at room temperature for 1 h. Strong change in colours was observed upon mixing solutions of the donors with the PA acceptor. The resulting solutions were allowed to stand at room temperature. The formed crystals were isolated, filtered off, and washed with the minimum given solvent to obtain the pure products. The crystals were then collected and dried in vacuo for 48 h. The obtained crystals were characterized by spectroscopy (UV-Vis, IR, Raman, and ^{1}H NMR), elemental and thermal analysis. The TEA-PA, Hyd-PA, TSC-PA, Phy-PA, and Pyr-PA crystals have a yellowish brown, orange, golden yellow, metallic silver, and yellow colour, respectively.

Stoichiometric determination

To determine the stoichiometry of the CT interactions in solution-state, various molar ratios were examined by spectrophotometric titration measurements. A 0.25, 0.50, 0.75, 1.00, 1.50, 2.0, 2.50, 3.00, 3.50, or 4.00 ml of a standard solution of the PA acceptor in methanol solvent was added to 1.00 ml of each donor at 5.0×10^{-4} M, dissolved in the same solvent. The final volume of the mixture was 5 ml. The concentration of the acceptor (C_a) varied from 0.25×10^{-4} M to 4.00×10^{-4} M, whereas the concentration of the donor (C_d) was maintained at 5.0×10^{-4} M to produce solutions with a molar ratio of donor:acceptor that varied from 4:1 to 1:4. The absorbance of each complex was plotted against the volume of the added acceptor.

For ascertaining the constituents, purity, and compositions of the synthesized solid complexes, elemental analyses (C, H, and N) were determined with the Micro analyser Perkin-Elmer CHN 2400 (USA) at Cairo University, Egypt.

Physical measurements

All the electronic absorption spectral measurements were recorded in methanol over a wavelength range of 200–800 nm using a Perkin-Elmer Lambda 25 UV-Vis double-beam spectrophotometer at Taif University, Saudi Arabia.

The IR absorption spectra of the solid CT complexes were measured as KBr discs within the range of 4000–400 cm^{-1} on a Shimadzu FT-IR spectrophotometer (Japan) at Taif University, Saudi Arabia.

The Raman laser spectra were performed on a Bruker FT-Raman spectrophotometer (Germany) equipped with a 50 mW laser at Taif University, Saudi Arabia.

^{1}H NMR spectra were collected by the Analytical Centre at King Abdul Aziz University, Saudi Arabia, on a Bruker DRX-250 spectrometer operating at 600 MHz. The measurements were performed

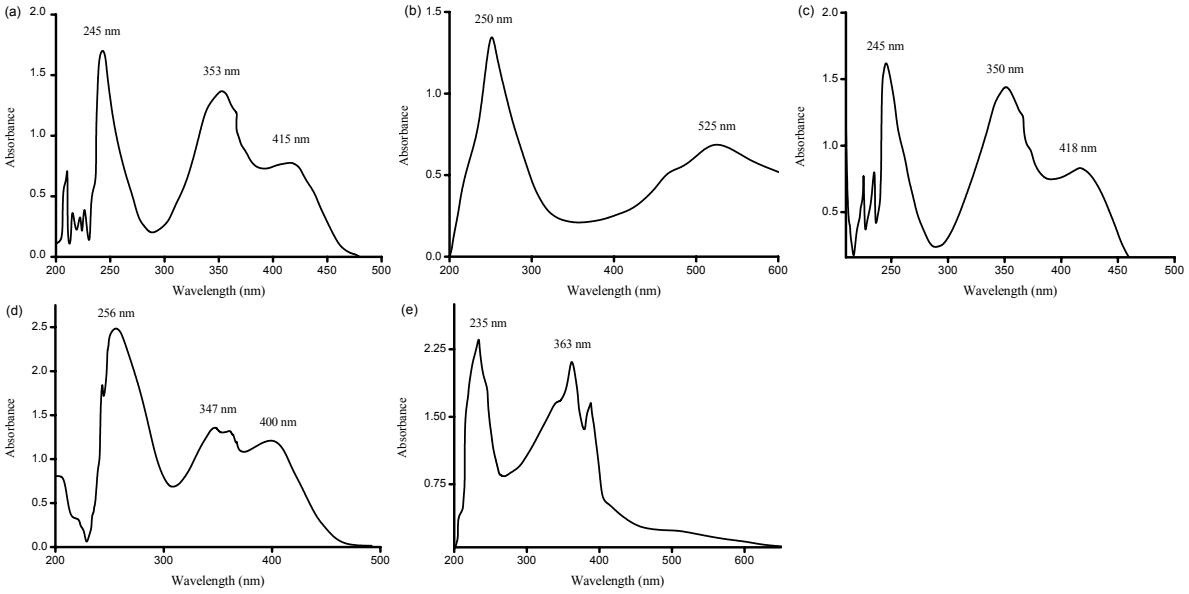

Fig. 2 Electronic absorption spectra of the reported CT complexes: (a) Hyd-Pa, (b) TEA-PA, (c) Phy-PA, (d) TSC-PA, (e) Pyr-PA.

at ambient temperature using DMSO-d_6 (dimethylsulphoxide, d_6) as a solvent and tetramethylsilane as an internal reference.

Thermogravimetric analysis (TG) was carried out under nitrogen atmosphere between room temperature and 800 °C using a Shimadzu TGA-50H thermal analyser (Japan) in the Central Lab at the Ain Shams University, Egypt.

An optical light microscope (OLM) instrument (model Meiji 7800 Techno Microscopy) was used to observe the morphological properties of the obtained crystals.

Calculations

The formation constant (K) and the molar extinction coefficient (ε) were determined spectrophotometrically using the 1:1 Benesi-Hildebrand equation[19] for the (1:1) CT complexes (with TEA, TSC, Phy, and Pyr donors) or the 1:2 modified Benesi-Hildebrand equation[20] for the (1:2) CT complexes (with Hyd donor). The spectroscopic data were used to calculate the energy of the interaction (E_{CT})[21], the oscillator strength (f)[22], the transition dipole moment (μ)[23], and the standard free energy (ΔG^*)[24] for the CT complexes in solution, using the equations described elsewhere in the literature.

Two different methods were employed to evaluate the kinetic-thermodynamic parameters in solid state: the Coats-Redfern method and the Horowitz-Metzger method. The kinetic-thermodynamic data were used to calculate the activation energy (E^*), the frequency factor (A), the enthalpy of activation (H^*), the entropy of activation (S^*), and the Gibbs free energy of activation (G^*) in the solid state using the Coats-Redfern[25] and Horowitz-Metzger methods[26].

RESULTS AND DISCUSSION

UV-Vis spectroscopy

The UV-Vis absorption spectra of the synthesized complexes (TEA-PA, Hyd-PA, TSC-PA, Phy-PA, and Pyr-PA) in solution mode were recorded in the range 200–800 nm (Fig. 2). These spectra indicated the presence of strong bands that correspond to the CT interactions. The spectrum of each complex was characterized by strong absorption bands appearing at: 250 and 525 nm for TEA complex; 245, 353, and 415 nm for Hyd complex; 256, 347, and 400 nm for TSC complex; 245, 350, and 418 nm for Phy; and 235 and 363 nm for Pyr complex.

Stoichiometry in solution

Fig. 3 shows the spectrophotometric titration curves for the reported CT complexes. The results show that the largest interaction between each donor and PA acceptor occurred at a donor:acceptor ratio of 1:2 for Hyd donor and of 1:1 for TEA, TSC, Phy, and Pyr donors. Thus the structures of the formed CT complexes were formulated to be $[(TEA^+)(PA^-)]$, $[(Hyd^+)(PA^-)_2]$, $[(TSC^+)(PA^-)]$,

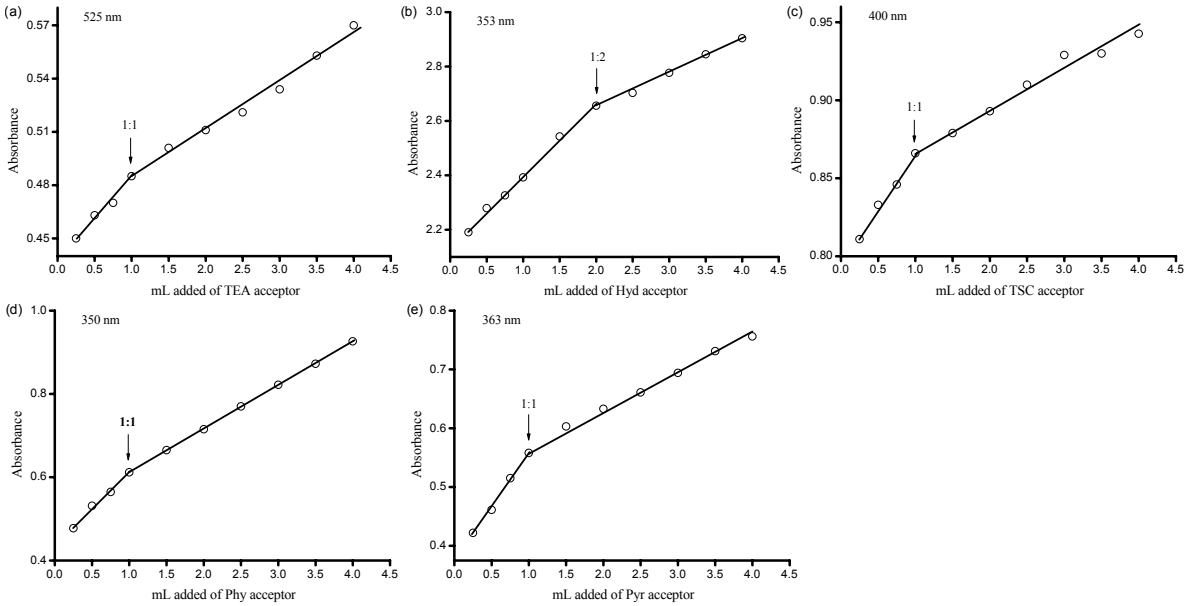

Fig. 3 Spectrophotometric titration curves for the reported CT complexes: (a) TEA-PA, (b) Hyd-Pa, (c) TSC-PA, (d) Phy-PA, (e) Pyr-PA.

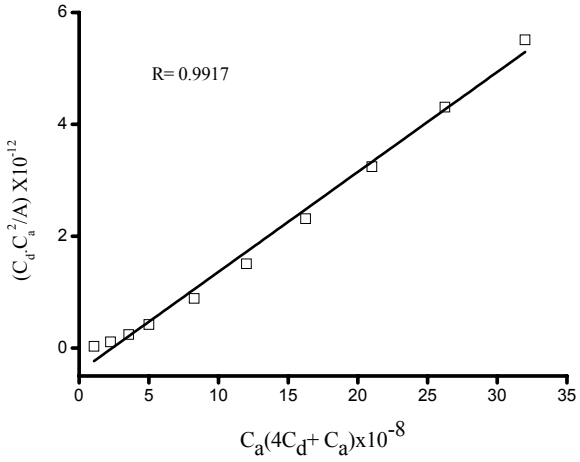

Fig. 4 The 1:2 Benesi-Hildebrand plot for Hyd-PA system.

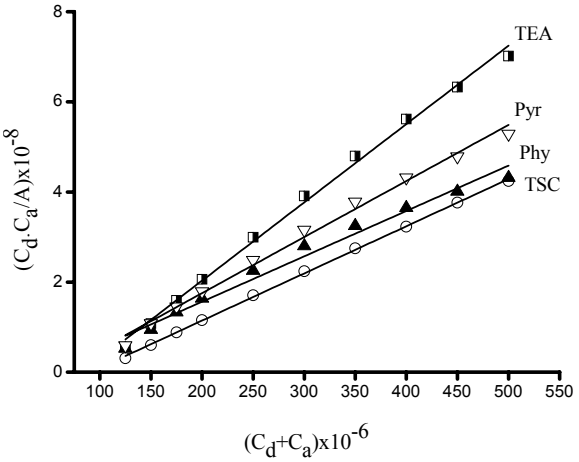

Fig. 5 The 1:1 Benesi-Hildebrand plots for TEA-PA, TSC-PA, Phy-PA, and Pyr-PA systems.

$[(Phy^+)(PA^-)]$, and $[(Pyr^+)(PA^-)]$. These stoichiometries agree quite well with the elemental analyses of the formed solid complexes.

Comparison of the spectroscopic data

Fig. 4 and Fig. 5 show representative 1:2 and 1:1 Benesi-Hildebrand plots, respectively, whereas Table 1 lists the values of the spectroscopic data (K, ε, f, μ, E_{CT}, and ΔG^*). The obtained data led to the following observations: (1) It was observed from Fig. 4 and Fig. 5 that the correlation coefficient (r) value for the straight lines was found to be greater than 0.99. (2) In general, the 1:2 complexes exhibit high values for K. The complex containing the Hyd donor shows higher K value, indicating a strong interaction between the Hyd-PA pairs, and confirms a high stability of the prepared complex. (3) The value of K for the TEA-PA complex is the highest value than other 1:1 complexes, reflecting the higher powerful electron donation ability for TEA. (4) The stability of the 1:1 complexes increases in the following order: Pyr-PA < Phy-PA < TSC-PA < TEA-PA. (5) The Hyd-PA complex shows higher

Table 1 Spectral properties of the donor-PA CT complexes at 298 K.

Property	1:1 complexes				
	TEA-PA	TSC-PA	Phy-PA	Pyr-PA	Hyd-PA
λ_{max} (nm)	525	400	350	363	353
Formation constant K (l/mol)	221.04×10^4	168.55×10^4	119.61×10^4	109.41×10^4	42.13×10^7
Extinction coefficient ε_{max} (l mol $^{-1}$ cm^{-1})	100.0×10^4	80.65×10^4	57.81×10^4	96.16×10^4	560×10^4
Energy value E_{CT} (eV)	3.55	3.43	2.37	3.11	6.05
Oscillator strength f	10.79	11.61	3.12	10.38	67.33
Dipole moment μ (D)	2.83	2.99	1.86	2.97	3.53
Free energy ΔG^* (kJ/mol)	-3.62×10^4	-3.55×10^4	-3.47×10^4	-3.45×10^4	-4.35×10^4

values of both μ and f, which indicates a strong interaction between the Hyd-PA pairs with relatively high probabilities of CT transitions. (6) The data also revealed that the complex containing the Hyd donor exhibits a very high ε value. (7) The ΔG^* values for all complexes are negative, indicating that the interaction between the donors and the PA acceptor is spontaneous. (8) The donation from the nitrogen moieties to PA acceptor in decreasing order is as follows: Hyd > TEA > TSC > Phy > Pyr.

Basicity effect on the stability of CT complexes

The comparison between the relative basicity of all the nitrogen moieties (TEA, Hyd, TSC, Phy, and Pyr) is discussed on the bases of evaluation the strength of the acidities of the conjugate acids of the bases (these conjugate acids are often 'onium' cations). The resulting pK_a's (K_a is the acid dissociation constant) are proportional to the base strength of the bases. The pK_a values of these bases are TEA, 10.8; Hyd, 8; TSC, 10; Phy, 8.79; Pyr, 5.2, (NH_3, 9.3; as reference)[27]. The low basicity of Pyr is based on the fact that sp^3-hybridized nitrogen is more basic than sp^2-hybridized nitrogen since the lone pair in the latter is closer to the positive nucleus and thus less available for donation. On the other hand, the week basicity of Hyd was attributed to the α effect, in which the neighbour nitrogen attracts the lone pair of electrons of the other nitrogen; while in the Phy, the benzene ring decreases the α effect due to electron donating phenyl group; hence the Phy is slightly more basic than Hyd. In TSC, the α effect is much lower than Hyd and Phy due to the presence of tautomerized thiocarbonyl group which is more powerful attracting the hydrogen of the NH_2 group by hydrogen bonding if compared to the benzene ring. Finally, TEA is the more basic nitrogen compound, because it has a sp^3 hybridized nitrogen with three electron repealing groups, which increases the power of the lone pair of electrons instead of the α effect. Hence the basicity of the nitrogen moieties in decreasing order are as follows: TEA > TSC > Phy > Hyd > Pyr. This ordering agrees well with the stability of the formed 1:1 complexes (TEA-PA > TSC-PA > Phy-PA > Pyr-PA).

CHN analysis

The percentage of composition of the elements (C, H, and N), molar ratio, and colour of the CT complexes are shown in Table 2. The experimental and calculated values of C, H, and N agree with each other and indicate that the obtained complexes are free from impurities. The stoichiometry of the PA acceptor complexes with the Hyd donor was found to have a 1:2 ratio, whereas its complexes with the TMA, TSC, Phy and Pyr

Table 2 Analytical and physical data of the reported CT complexes.

Complex	Molecular formula	Molecular weight (g/mol)	Elemental analyses						Molar ratio	Colour
			C (%)		H (%)		N (%)			
			Found	Calc.	Found	Calc.	Found	Calc.		
$[(Hyd^+)(PA^-)_2]$	$C_{12}H_{10}N_8O_{14}$	490.25	29.44	29.40	2.10	2.06	22.82	22.86	1:2	Orange
$[(TEA^+)(PA^-)]$	$C_{12}H_{18}N_4O_7$	330.29	43.60	43.64	5.45	5.49	17.03	16.96	1:1	Yellowish brown
$[(TSC^+)(PA^-)]$	$C_7H_8N_6O_7S$	320.24	26.21	26.25	2.48	2.52	26.30	26.25	1:1	Golden yellow
$[(Phy^+)(PA^-)]$	$C_{12}H_{11}N_5O_7$	337.25	42.79	42.74	3.33	3.29	20.80	20.77	1:1	Metallic silver
$[(Pyr^+)(PA^-)]$	$C_{11}H_8N_4O_7$	308.20	42.85	42.87	2.66	2.62	18.11	18.18	1:1	Yellow

Table 3 Assignments of the characteristic IR and Raman spectral bands (cm^{-1}) for the reported CT complexes.

Complex	$\delta(NH_3^+)_{def}$		$\delta(NH_3^+)_{sym}$		ϱ (NH_3^+)		$\nu(^+NH)$	
	IR	Raman	IR	Raman	IR	Raman	IR	Raman
$[(Hyd^+)(PA^-)_2]$	1630	1570	1316	1342	788	826	–	–
$[(TSC^+)(PA^-)]$	1631	1566	1339	1332	790	824	–	–
$[(Phy^+)(PA^-)]$	1569	1614	1340	1308	853	860	–	–
$[(TEA^+)(PA^-)]$	–	–	–	–	–	–	3022	3038
$[(Pyr^+)(PA^-)]$	–	–	–	–	–	–	3074	3110

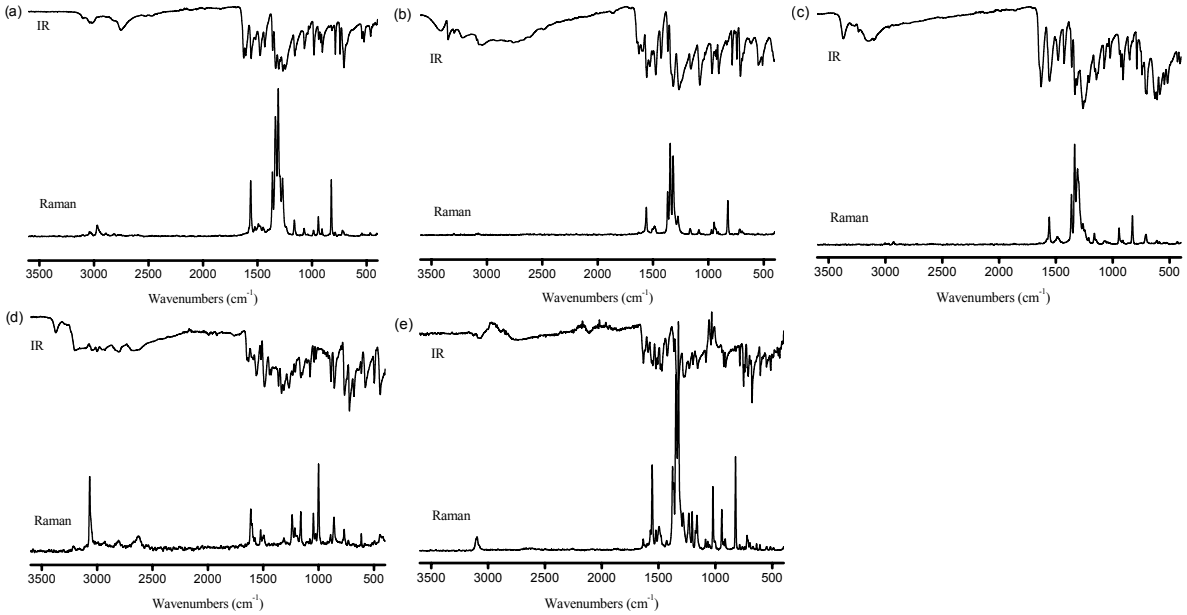

Fig. 6 IR and Raman laser spectra of the reported CT complexes.

donors was found to have a 1:1 ratio. Thus the prepared CT complexes were formulated as $[(TEA^+)(PA^-)]$, $[(Hyd^+)(PA^-)_2]$, $[(TSC^+)(PA^-)]$, $[(Phy^+)(PA^-)]$, and $[(Pyr^+)(PA^-)]$. The formation of 1:1 and 1:2 CT complexes was strongly supported by UV-Vis, IR, Raman, ^{1}H NMR, and thermal analysis. These stoichiometry values agree quite well with the data obtained from the spectrophotometric titrations.

Vibrational spectroscopy

Table 3 lists the peak assignments for the characteristic IR and Raman bands for the synthesized CT complexes. The full IR and Raman spectra of the complexes are illustrated in Fig. 6. The IR/Raman spectra of the Hyd, TSC, and Phy complexes revealed the appearance of the main characteristic absorption bands that result from the stretching and bending deformation of the $(-NH_3^+)$ group; $\nu_{def}(NH_3^+)$, $\delta_{sym}(NH_3^+)$, and $\varrho(NH_3^+)$ vibrations. These vibrations occur at approximately 1600, 1300, and 800 cm^{-1}, respectively. The presence of these bands confirmed that the complexation occurs through the protonation of the $(-NH_2)$ group of the donors via a proton-transfer phenomenon from the PA acceptor to the basic centre ($-NH_2$ group) of the donors to form NH_3^+ ammonium [16–18]. In the IR/Raman spectra of the TMA and Pyr complexes, the characteristic bands observed at (IR/Raman) 3022/3038 cm^{-1} for TMA complex and 3074/3110 cm^{-1} for Pyr complex, which are assigned to ($^+$NH) asymmetric and symmetric stretching vibration, respectively. This observation indicates that the complexation occurs through the formation of hydrogen bonding between these two donors and the PA acceptor molecules [8, 9, 28].

^{1}H NMR spectroscopy

The 600 MHz ^{1}H NMR spectra of the CT complexes were measured in DMSO-d_6 solvent at room temperature using tetramethylsilane as internal standard. The positions of chemical shifts of the different kinds

of protons in these complexes include the following:

TEA complex: $\delta = 1.59$ (t, 9H, $3\,CH_3$), 3.13 (q, 6H, $3\,CH_2$), 5.49 (s, 1H, HN^+), 8.49 (s, 2H, Ar-H of picric acid).

Hyd complex: $\delta = 5.26$ (s, 6H, $2(H_3N^+)$), 8.82 (s, 4H, Ar-H of picric acid).

TSC complex: $\delta = 6.77$ (s, 1H, CSNH), 6.95 (s, 3H, H_3N^+), 8.79 (s, 2H, Ar-H of picric acid), 10.25 (s, 2H, $CSNH_2$).

Phy complex: $\delta = 6.77$ (d, 2H, C_2, C_6 benzene ring protons), 6.85 (d, 1H, C_4 benzene proton), 6.91 (m, 2H, C_3, C_5 benzene protons), 7.49 (s, 3H, H_3N^+), 8.79 (s, 2H, Ar-H of picric acid).

Pyr complex: $\delta = 5.49$ (s, 1H, HN^+), 6.63 (m, 2H, C_3, C_5 pyridine protons), 6.95 (d, 1H, C_4 pyridine proton), 7.54 (d, 2H, C_2, C_6 pyridine protons), 8.57 (s, 2H, Ar-H of picric acid).

The signal of (−OH), which is observed at δ approximately 11.94 ppm in the spectrum of free PA, is absence in the spectra of these complexes. Instead, the peaks appeared at 5.26 (TEA), 6.95 (TSC) and 7.49 ppm (Phy), are assigned to NH_3^+ protons. These data indicate that the amino and (−OH) groups are involved in the formation of the CT complex between these donors and the PA acceptor. The band observed at 5.49 ppm in the TEA and Pyr complexes was attributed to the formation of ($^+$NH), indicates the deprotonation from the PA acceptor to these donors.

Table 4 Thermal decomposition data for the reported CT complexes.

Compound	Stages	TG range (°C)	TG% mass loss		Lost species
			Found	Calc.	
$[(Hyd^+)(PA^-)_2]$	I	135–440	75.55	76.63	Hyd + 1.5PA
	II	440–800	23.28	23.37	0.5PA
$[(TEA^+)(PA^-)]$	I	215–460	69.15	69.36	PA
	II	460–800	19.68	19.74	$C_3H_{15}N$
	Residue	–	10.08	10.90	3C
$[(TSC^+)(PA^-)]$	I	100–490	71.02	71.54	PA
	II	490–800	17.88	18.46	CH_5N_3
	Residue	–	9.75	10.0	S
$[(Phy^+)(PA^-)]$	I	200–800	99.75	100.0	Phy + PA
$[(Pyr^+)(PA^-)]$	I	125–265	14.71	14.93	NO_2
	II	265–515	47.65	47.71	$C_3H_3N_2O_5$
	III	515–800	25.70	25.67	Pyr
	Residue	–	11.50	11.69	3C

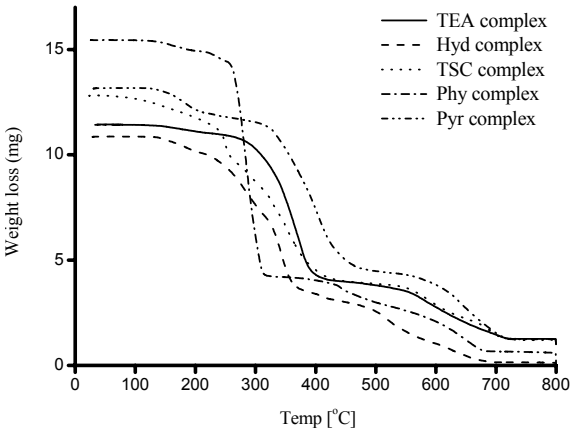

Fig. 7 Thermograms of the reported CT complexes.

Comparison of the thermograms

The comparative study of thermograms for these complexes was carried out by TG under a static air atmosphere in the temperature range 25–800 °C. The measurements were carried out using 11.44, 10.85, 12.80, 15.44, and 13.14 mg for TEA, Hyd, TSC, Phy, and Pyr complex, respectively. The thermoanalytical data for these complexes are collected in Table 4, while their thermograms are presented in Fig. 7. Analyses of the TG thermograms of the synthesized CT complexes provided the following observations: (1) The observed weight loss is in good agreement with the theoretical ones. (2) Decomposition of the complexes began at approximately 215, 135, 100, 200, and 125 °C for TEA, Hyd, TSC, Phy, and Pyr complex, respectively, and finished at approximately 800 °C. (3) The thermogram of the Phy complex exhibit it decomposes in one step. (4) The complexes of TEA, Hyd, and TSC exhibit two decomposition steps. (5) The complex containing the Pyr donor was thermally decomposed in nearly three decomposition steps. (6) Generally, the first decomposition step is corresponded to the removal of the acceptor moiety. (7) Decomposition of TEA and Pyr complexes led to residual carbon as a final product. (8) Interestingly, the thermal degradation of the TSC complex resulted in a residual sulphur atoms remaining as the final product. (9) The overall loss of mass is 89% for TEA-PA, 99% for Hyd-PA, 89% for TSC-PA, 99.8% for Phy-PA, and 88% for Pyr-PA. The calculated values is in excellent agreement with the total weight observed.

Comparison of the thermodynamic data

The thermodynamic parameters (E^*, A, H^*, S^*, and G^*) associated with the CT complexes were evaluated graphically (Fig. 8) by employing the Coats-Redfern and Horowitz-Metzger methods, and the evaluated data are listed in Table 5. The obtained data led to the following observations: (1) The thermodynamic data obtained from the two methods are comparable and can be considered in good agreement with each other; (2) The E^* value for the $[(Hyd^+)(PA^-)_2]$ complex is higher compared to the

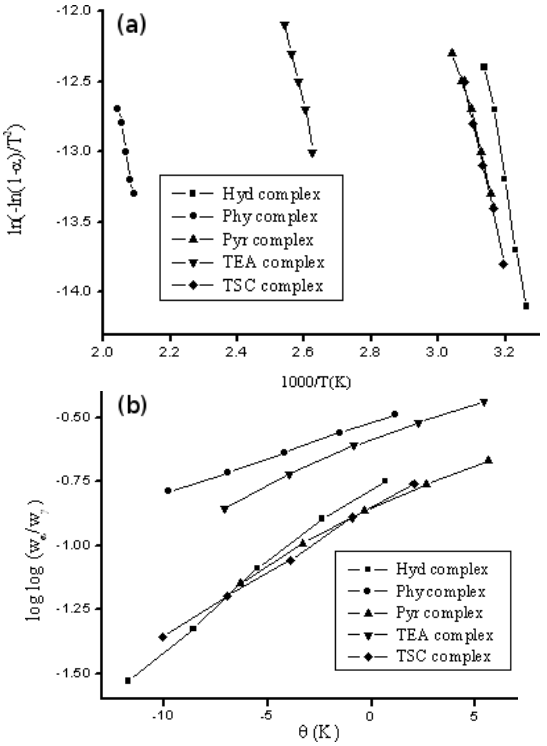

Fig. 8 Thermodynamic plots for the reported CT complexes; (a) Coats-Redfern equation; (b) Horowitz-Metzger equation.

Table 5 Kinetic data of thermal decomposition determined using the Coats-Redfern (CR) and Horowitz-Metzger (HM) methods.

Complex	Method	Parameters†					r
		E^*	A	ΔS^*	ΔH^*	ΔG^*	
$[(Hyd^+)(PA^-)_2]$	CR	116	1.20×10^{17}	83	110	85	0.9965
	HM	121	1.10×10^{19}	118	114	83	0.9961
$[(TEA^+)(PA^-)]$	CR	94	3.39×10^{9}	−62	82	101	0.9971
	HM	92	2.46×10^{10}	−50	91	100	0.9959
$[(TSC^+)(PA^-)]$	CR	85	7.78×10^{10}	−38	81	90	0.9944
	HM	86	2.38×10^{12}	−30	82	88	0.9920
$[(Phy^+)(PA^-)]$	CR	108	5.55×10^{9}	−65	102	132	0.9955
	HM	115	7.10×10^{10}	−43	110	130	0.9988
$[(Pyr^+)(PA^-)]$	CR	72	1.14×10^{9}	−70	66	86	0.9945
	HM	74	2.80×10^{10}	−48	72	84	0.9932

† Units: E^* in kJ/mol, A in s^{-1}, ΔS^* in J mol^{-1} K^{-1}, ΔH^* and ΔG^* in kJ/mol.

other complexes, which indicates the higher thermal stability of this complex; (3) The E^* values of the complexes occur in a decreasing order as follows. Hyd > Phy > TEA > TSC > Pyr; and (4) The ΔS^* values of the complexes decrease in the following order: Hyd > TSC > Phy > TEA > Pyr.

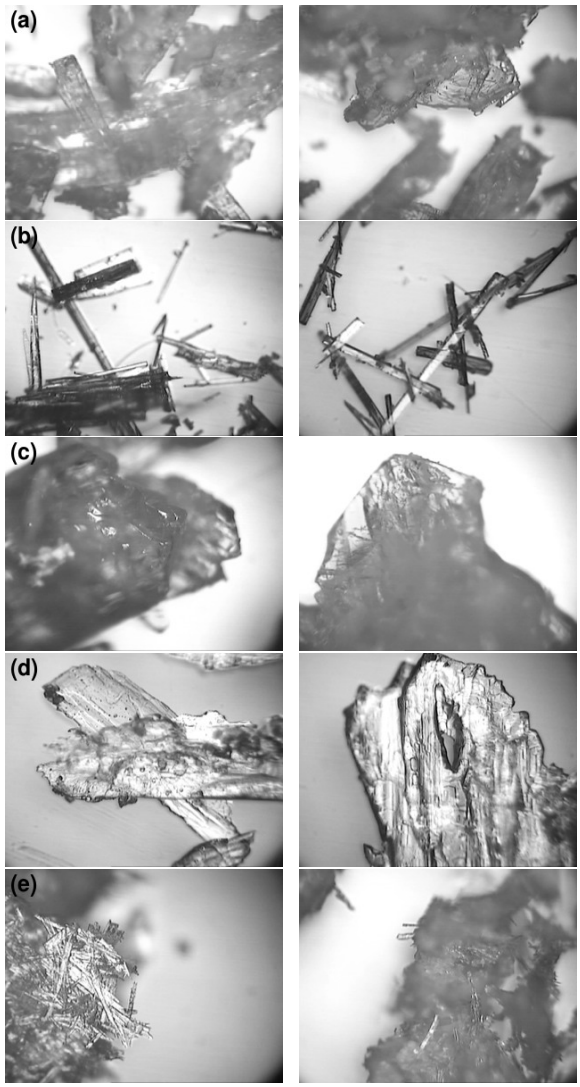

Fig. 9 OLM micrographs of (a) the TEA-PA complex, (b) the Hyd-PA complex, (c) the TSC-PA complex, (d) the Phy-PA complex, and (e) the Pyr-PA complex.

Microstructure properties

Optical light microscope (OLM) provides colourful micrographs. Colour is an advantage for residue identification and characterization, and can also help to recognize potential contamination. OLM was employed to observe the morphology of the prepared complexes. Fig. 9 illustrates multiple OLM pictures of the CT complexes. The complexation of PA acceptor with the different nitrogen moieties leads to very interesting microstructures. The high quality and well-focused micrographs indicate that these complexes have well-defined morphologies. The obtained complexes are crystalline, as indicated

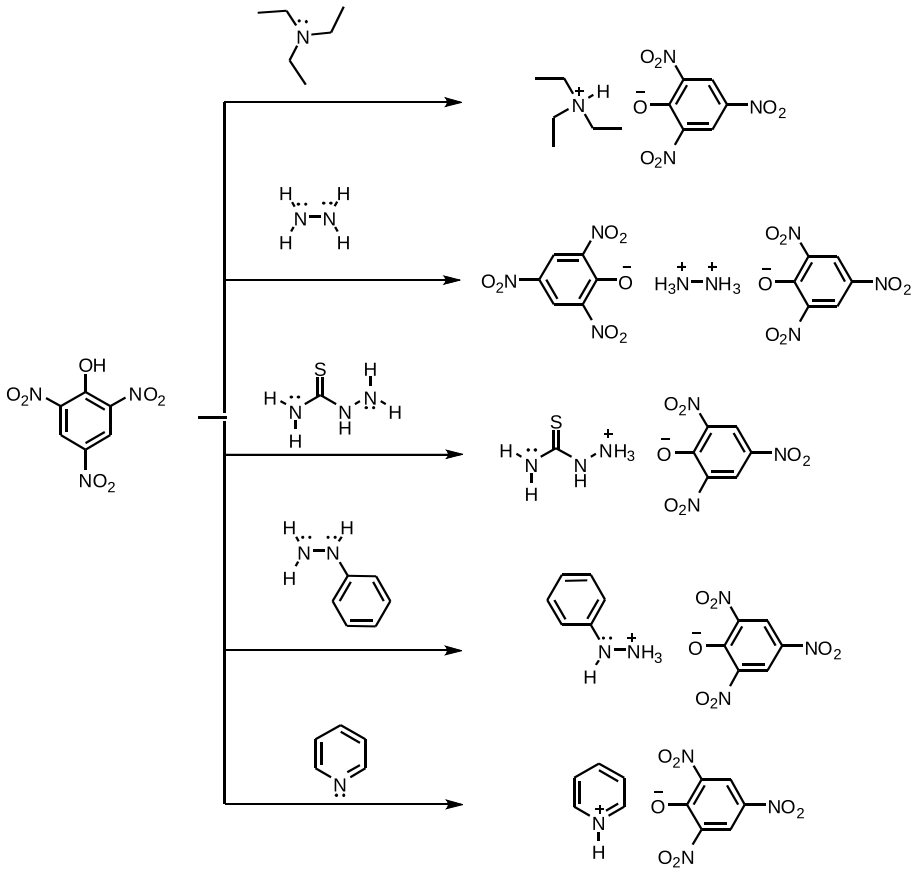

Fig. 10 Proposed structural formula of the synthesized CT complexes.

by the formation of single-phases with well-defined shape. Visible change in the morphology is observed between the different CT complexes.

Structural interpretation

The structures of the synthesized CT complexes are confirmed by CHN analysis, spectrophotometric titration, spectral data, and thermal analysis. The data obtained by these techniques are in agreement with each other. Fig. 10 illustrated the proposed chemical structures of the synthesized CT complexes.

CONCLUSIONS

Intermolecular CT complexes between the nitrogen moieties of TEA, Hyd, TSC, Phy, and Pyr as donors with picric acid (PA) as an acceptor have been structurally, thermally, and morphologically investigated in MeOH solvent at room temperature. The obtained CT complexes were isolated and characterized by spectroscopy (IR, Raman, ^{1}H NMR, and UV-Vis) elemental and thermal analyses. Spectrophotometric titration and elemental analyses indicate that the CT complexes are formed based on a 1:1 stoichiometric ratio, except for Hyd donor (1:2 ratio). IR, Raman, and ^{1}H NMR revealed evidence of significant intermolecular hydrogen bonding interactions between each donor and PA acceptor based on their characteristic shifts. Thermal experimental data suggests that the formation of the complexes was spontaneous, stable, and exothermic. Significant changes in the morphology of these complexes were observed using optical light microscope.

Acknowledgements: The project was financially supported by King Saud University, Vice Deanship of Research Chairs.

REFERENCES

1. Mulliken RS (1950) Structures of complexes formed by halogen molecules with aromatic and with oxygenated solvents. *J Am Chem Soc* **72**, 600–8.
2. Foster R (1969) *Charge Transfer Complexes*, Academic press, London.
3. Mulliken RS (1952) Molecular compounds and their spectra II. *J Am Chem Soc* **74**, 811–24.

4. Roy T, Dutta K, Nayek MK, Mukherjee AK, Banerjee M, Seal BK (1999) Study of a novel reaction between *N*,*N*′-diphenylthiourea and *p*-chloranil through a charge-transfer intermediate. *J Chem Soc Perkin Trans 2* **1999**, 2219–23.
5. Slifkin AM (1971) *Charge-Transfer Interaction of Biomolecules*, Academic Press, New York.
6. Roy DK, Saha A, Mukherjee AK (2005) Interaction of 2,3-dichloro-1,4-naphthoquinone with *n*-butylamine in halocarbon solvents. *Spectrochim Acta A* **61**, 1729–35.
7. Dozal A, Keyzer H, Kim HK, Wang WW (2000) Charge transfer complexes of K vitamins with several classes of antimicrobials. *Int J Antimicrob Agents* **14**, 261–5.
8. Pandeeswaran M, El-Mossalamy EH, Elango EH (2009) Spectroscopic studies on the dynamics of charge-transfer interaction of pantoprazole drug with DDQ and iodine. *Int J Chem Kinet* **41**, 787–99.
9. Khan IM, Ahmad A, Ullah MF (2011) Synthesis, crystal structure, antimicrobial activity and DNA-binding of hydrogen-bonded proton-transfer complex of 2,6-diaminopyridine with picric acid. *J Photochem Photobiol B* **103**, 42–9.
10. Khan IM, Ahmad A, Kumar S (2013) Synthesis, spectroscopic characterization and structural investigations of a new charge transfer complex of 2,6-diaminopyridine with 3,5-dinitrobenzoic acid: DNA binding and antimicrobial studies. *J Mol Struct* **1035**, 38–45.
11. Yakuphanoglu F, Arslan M (2004) Determination of electrical conduction mechanism and optical band gap of a new charge transfer complex: TCNQ-PANT. *Solid State Comm* **132**, 229–34.
12. Andrade SM, Costa SMB, Pansu R (2000) Structural changes in W/O triton X-100/cyclohexane-hexanol/water microemulsions probed by a fluorescent drug piroxicam. *J Colloid Interface Sci* **226**, 260–8.
13. Krishnamoorthy G, Dogra SK (2000) Excited state intramolecular proton transfer in 2-(2′-hydroxyphenyl)-3H-imidazo[4,5-b]pyridine: effect of solvents. *J Lumin* **92**, 91–102.
14. Smith G, Bott RC, Rae AD, Willis AC (2000) The modulated crystal structure of the molecular adduct of 2,4,6-trinitrobenzoic acid with 2,6-diaminopyridine. *Aust J Chem* **53**, 531–4.
15. Refat MS, Adam AMA, Sharshar T, Saad HA, Eldaroti HH (2014) Utility of positron annihilation lifetime technique for the assessment of spectroscopic data of some charge-transfer complexes derived from *N*-(1-naphthyl)ethylenediamine dihydrochloride. *Spectrochim Acta A* **122**, 34–47.
16. Refat MS, Ismail LA, Adam AMA (2015) Shedding light on the photostability of two intermolecular charge-transfer complexes between highly fluorescent bis-1,8-naphthalimide dyes and some π-acceptors: A spectroscopic study in solution and solid states. *Spectrochim Acta A* **134**, 288–301.
17. Eldaroti HH, Gadir SA, Refat MS, Adam AMA (2014) Charge-transfer interaction of drug quinidine with quinol, picric acid and DDQ: Spectroscopic characterization and biological activity studies towards understanding the drug-receptor mechanism. *J Pharmaceut Anal* **4**, 81–95.
18. Adam AMA, Refat MS, Saad HA (2013) Utilization of charge-transfer complexation for the detection of carcinogenic substances in foods: Spectroscopic characterization of ethyl carbamate with some traditional π-acceptors. *J Mol Struct* **1037**, 376–92.
19. Benesi HA, Hildebrand JH (1949) A spectrophotometric investigation of the interaction of iodine with aromatic hydrocarbons. *J Am Chem Soc* **71**, 2703–7.
20. Abu-Eittah R, Al-Sugeir F (1976) Charge-transfer interaction of bithienyls and some thiophene derivatives with electron acceptors. *Can J Chem* **54**, 3705–12.
21. Briegleb G (1964) Electron affinity of organic molecules. *Angew Chem Int Ed* **3**, 617–32.
22. Tsubomura H, Lang RP (1961) Molecular complexes and their spectra XIII. Complexes of iodine with amides, diethyl sulfide and diethyl disulfide. *J Am Chem Soc* **83**, 2085–92.
23. Rathore R, Lindeman SV, Kochi JK (1997) Charge-transfer probes for molecular recognition via steric hindrance in donor-acceptor pairs. *J Am Chem Soc* **119**, 9393–404.
24. Aloisi GG, Pignataro S (1973) Molecular complexes of substituted thiophens with σ and π acceptors. Charge transfer spectra and ionization potentials of the donors. *J Chem Soc Faraday Trans* **69**, 534–9.
25. Coats AW, Redfern JP (1964) Kinetic parameters from thermogravimetric data. *Nature* **201**, 68–9.
26. Horowitz HH, Metzger G (1963) A new analysis of thermogravimetric traces. *Anal Chem* **35**, 1464–8.
27. William MH (2014) *Handbook of Chemistry and Physics*, 95th edn, Chemical Rubber Publishing Company, Cleveland.
28. Manikandan M, Mahalingam T, Hayakawa Y, Ravi G (2013) Synthesis, structural, spectroscopic and optical studies of charge transfer complex salts. *Spectrochim Acta A* **101**, 178–83.